P2.25

MOISTURE CORRESPONDENCE BETWEEN LOWER AND UPPER TROPOSPHERE OVER OCEANS USING AIRS OBSERVATIONS

Hengchun Ye[1], Department of Geography and Urban Analysis, California State University, Los Angeles
E. J. Fetzer, S. Granger, S-Y Lee, E. T. Olsen, B. H. Lambridgtsen and L. Chen
Jet Propulsion Laboratory, California Institute of Technology, Pasadena, CA

1. INTRODUCTION

The Atmospheric Infrared Sounder (AIRS) mounted on Aqua space craft measures vertical profiles of air temperature and humidity using both microwaves and infrared irradiance (Pagano et al. 2003; Lambrigtsen and Lee 2003; Susskind et al. 2003; Autmann et al. 2003). The AIRS' level III data that provide gridded values of 1° latitude by 1° longitude for the highest temporal resolution of twice per day became available recently (Granger et al. 2005). This level III data were derived from the level II Version 4.0 AIRS retrieval algorithm (Fetzer et al 2005; Ye et al. 2005).

This study uses this level III AIRS moisture profile data to reveal geographical correspondences of atmospheric moisture content between the lower and upper troposphere.

2. METHODS

The daily gridded AIRS atmospheric specific humidity over world oceans between 50ºS to 50ºN are used to derive three-day averages of vertical integrated moisture content for the two air columns: 1000mb-500mb (100mb, 925mb, 850mb, 700mb, 600mb, 500mb) and 500mb-100mb (400mb, 300mb, 250mb,200mb, 150mb, 100mb) for the six months of January to June 2005. The vertical integration of water vapor is based on the following equation: $w = \int_{p_1}^{p_2} q_i * \Delta p_i / g$

then singular value decomposition analysis (SVD) is performed to identify the teleconnections among grids between these two atmospheric layers. Thus the two fields analyzed in SVD are the moisture field below 500mb and the moisture field above 500mb. The time series of the resulting major SVD patterns are used to reveal the dominant mode of temporal variations ranging from daily to seasonal time scales.

3. RESULTS

Six major patterns produced by SVD are analyzed. They explained about 46.8% of total variance of the two moisture fields below and above 500mb.

The time series of pattern 1 shows a strong seasonal pattern of variation: the value peaks in early February and decreases gradually for the remaining 5 month (Figure 1). The PC1 for both below and above 500mb match closely.

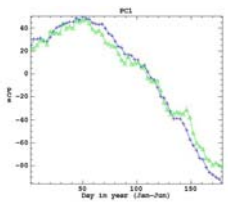

Figure 1. Time series of PC1 above (blue) and below (green) 500mb

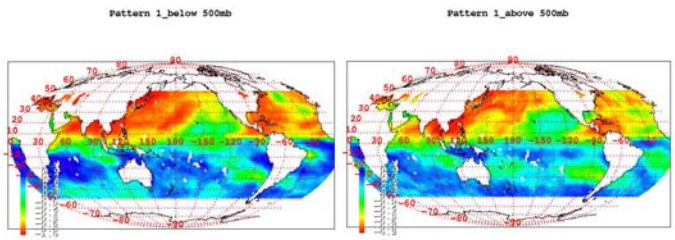

Figure 2. EOF of PC1 on moisture below (left) and above (right) 500mb

The spatial pattern of PC1 for both below and above 500mb match closely. This suggests that abundant moisture over the southern hemispheric tropical ocean is decreasing while these over the northern hemisphere is increasing starting in early February both below and above 500mb (Figure 2). One major difference between the two layers are found in the western South Pacific Ocean, around 20ºS extending from east coast of Australia to about 150ºW. In this region, the moisture in more abundant in the lower troposphere than the upper, thus more significant seasonal variations of moisture exist in the lower troposphere. A similar pattern to this (mirror image) is evident in the North Pacific Ocean where the lower atmospheric moisture also seems to have stronger seasonal variations. This may be related to the fact that moisture is discharged into these areas constantly throughout the year from land areas over upper troposphere. This phenomenon can be seen from daily moisture changes. Over the equatorial regions of eastern Pacific between 150ºW-120ºW, upper tropospheric moisture seems to have a stronger seasonal variation as shown in Figure 2.

Pattern 2 shows intraseasonal variations overlaid with a sesonal variation that peaked in early April (Figure 3). On daily scales, PC2 for lower tropospheric (blue) moisture has slightly different values compared to the upper troposphere (green). The major activities described by this pattern are over the eastern equatorial Pacific, the equatorial Atlantic Ocean, and the southern Indian Ocean (Figure 4). Variation of this pattern seems to be stronger over lower troposphere in most areas. However, in the area over the northern coast of Australia, and coast of southern Africa, the variations seems to be more noticeable on upper troposphere.

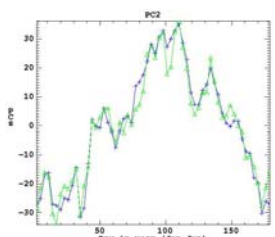

Figure 3. Time series of PC2

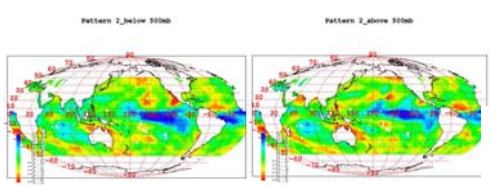

Figure 4. EOF of PC2 for moisture below (left) and above (right) 500mb.

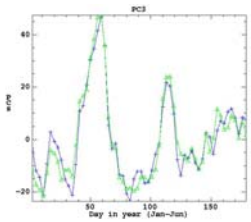

Figure 5. Time series of PC3 for below (blue) and above (green) 500mb

Figure 6. EOFs of PC3 for moisture field below (left) and above (right) 500mb

Pattern three shows an intraseasonal variation of about 50 days with a stronger cycle occurring over February and March (Figure 5). The pattern reveals sandwiched off-phase moisture changes over the middle and tropical Pacific Oceans. Activities seem to be of similar strengths between lower and upper troposphere, except over the western equatorial ocean where upper troposphere has a stronger variation amplitude (Figure 6).

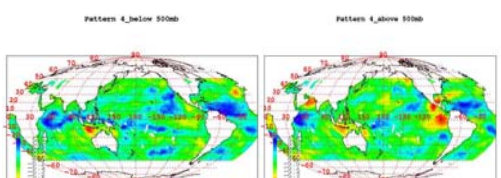

Figure 8. EOF of PC4 for moisture below (left) and above (right) 500mb

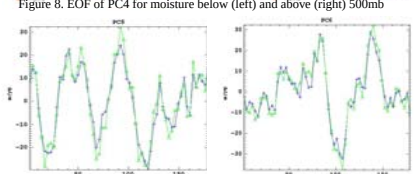

Figure 9. Time series of PC5 and PC6 for both moisture field

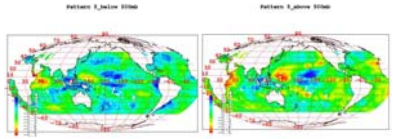

Figure 10. EOF of PC5 for moisture below (left) and above (right) 500mb

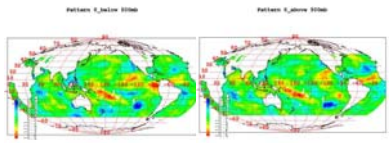

Figure 11. EOF of PC6 for moisture below (left) and above (right) 500mb

4. Conclusions

This study analyzed connections of moisture content between the lower and upper troposphere over global middle-latitude and tropical oceans for the time period of 6 month in 2005 using AIRS's level III data set. It is interesting to see that the dominant seasonal and intraseasonal variation patterns correspond well between lower and upper troposphere with stronger variability over the lower troposphere. As the variance of pattern decreases, poorer correspondence starts to show in some areas.

This study suggests that an universal moisture profile over oceans is in general a good assumption. Exceptions occur over certain geographical regions near to a landmass, where moisture profiles may be modified.

5. REFERENCES

Aumann, H. H., M. T. Chahine, C. Gautier, M. D. Goldberg, E. Kalnay, L. M. McMillin, H. Revercomb, P. W. Rosenkranz, W. L. Smith, D. H. Staelin, L. L. Strow and J. Susskind, 2003: AIRS/AMSU/HSB on the Aqua mission: design, science objectives, data products and processing system, IEEE Trans. Geosci. And Remote Sensing, 41, 253-264.

Fetzer, E. J., A. Eldering, E. F. Fishbein, T. Hearty, W. F. Iron and B. Kahn, 2005: Validation of AIRS/AMSU/HSB core products for data release version 4.0, March 8, 2005, JPL D-31448, 79 pages (http://disc.gsfc.nasa.gov/AIRS/index.shml).

Lambrigtsen, B. H.,, and S.-Y. Lee, 2003: Coalignment and synchronization of the AIRS instrument suite, IEEE Trans. Geosci, and Remote Sensing, 41, 343-351.

Pagano, T. S. H. H. Aumann, D. E. Hagan and K. Overoye, 2003: Prelaunch and in-flight radiometric calibration of the Atmospheric Infrared Sounder (AIRS), IEEE Trans. Geosci. and Remote Sensing, 41, 265-273.

Granger, S., Leroy, S.S., Manning, E.M., Fetzer, E.J., Oliphant, R.B., Braverman, A., Lee, S.Y., Lambrigtsen, B., 2004: Development of level 3 (gridded) products for the Atmospheric Infrared Sounder (AIRS), In *Proceedings of IGARSS 2004, 20-24 September 2004, Anchorage Alaska*

Ye, H., E. J. Fetzer, E. T. Olsen, A. Eldering, S. Granger, L. Chen, B. H. Lambrigtsen, E. Fishen, S.-Y. Lee, 2005: Structure of the lower atmosphere over the Pacific Ocean: information gained from AIRS observations. Ninth Symposium on Integrated Observing and Assimilation Systems for the Atmospherei, Oceans, and Land Surfaces (IOAS-AOLS), P1.4. American Meteorological Society.